JOURNAL OF MATERIALS SCIENCE **37** (2002) 1363–1376

Novel heat spreader coatings for high power electronic devices

K. JAGANNADHAM
Materials Science and Engineering, N. C. State University, Raleigh, NC 27695-7916, USA
E-mail: Jag_kasichainula@ncsu.edu

T. R. WATKINS, R. B. DINWIDDIE
High Temperature Materials Laboratory, Oak Ridge National Laboratory, Oak Ridge, TN 37831-6062, USA

A new set of heat spreader coatings consisting of multilayers of diamond/AlN/diamond were deposited on high heat capacity substrates of molybdenum and silicon nitride. Bonding of the heat spreaders to the device wafers using gold-tin eutectic solder was carried out after metallization layers of titanium, gold and copper were deposited on diamond. Prior to bonding, backside of the silicon wafers was also metallized with titanium, gold and copper and the gallium arsenide wafers with titanium, copper-germanium alloy and gold. Characterization of the multilayer diamond films was carried out by Raman spectroscopy, X-ray diffraction and scanning electron microscopy. The bonded wafers were tested for adhesion strength, resistance against peeling due to thermal cycling and failure under stress. Further, the bonded regions were characterized by scanning electron microscopy, energy dispersive spectroscopy and X-ray mapping of different elements. The heat spreader characteristics of the single layer diamond and the multilayer diamond substrates were tested by infrared imaging. The results illustrate that the multilayer diamond heat spreader coatings provide better heat dissipation and also possess better adhesion strength and resistance against peeling under thermal cycling. These novel multilayer diamond/AlN/diamond heat spreaders are expected to considerably improve the life of high frequency power devices. © *2002 Kluwer Academic Publishers*

1. Introduction

High frequency, high power electronic devices generate large thermal energy during operation of the device leading to a sharp raise in temperature and susceptibility to both electronic and mechanical failure [1–6]. These devices include among others microwave power devices, high power switches, and modern laser diodes that are built on semiconductor substrates such as silicon, gallium arsenide, silicon carbide and other wide band gap semiconductors. Progress in reduction in size of the active devices to submicron level with a corresponding increase in device density and frequency of operation is expected to lead to large increase in the heat dissipation. Therefore, it is important that better heat spreaders are built into the design of the electronic devices. Low cost, high reliability and high heat spreader characteristic substrates are explored currently for use in electronic industry. Among these, high thermal conductivity diamond [7, 8], moderately good thermal conductivity sintered aluminum nitride [9], low thermal expansion copper alloys [10, 11] and a variety of composite materials [12, 13] are currently explored.

Amongst other physical properties, high thermal conductivity, high dielectric constant, and high specific heat are used as important necessary characteristic features for an efficient heat spreader. Traditionally beryllium oxide is used as a heat spreader, however, newer materials are chosen to replace it because of the toxicity and high cost. Diamond, AlN and SiC are promising in this respect. The contributions to the thermal conductivity of these ceramic compounds is mostly from the lattice or phonons and any impurities responsible for phonon scattering will be detrimental and therefore high purity synthesis is an important constraint associated with their use. Aluminum nitride ceramic heat spreaders are used increasingly in place of toxic beryllium oxide substrates. For high frequency electronic power devices, however, diamond is a better heat spreader because of its higher thermal conductivity. However, the low specific heat is a disadvantage when diamond is used alone. To absorb the heat quickly and ensure that the temperature rise of the high frequency device is kept low, higher specific heat will be advantageous under nonsteady state conditions. Therefore, a higher specific heat substrate such as molybdenum or silicon nitride with diamond film deposited directly on it is expected to serve as a better heat spreader in high frequency devices.

In this paper, consideration is given to reliable design of the heat spreader substrates and bonding to the device

wafers. A new design of heat spreaders that is responsible for more effective and better dissipation of thermal energy generated by the high frequency power devices is presented. The processing steps including deposition of the coatings and bonding of the heat spreaders to the wafers, characterization, and testing of the multilayer structure are discussed.

2. Novel design of heat spreaders

The thermal conductivity of diamond close to room temperature is forty times that of GaAs and four to five times that of copper, aluminum nitride or silicon carbide. Low-pressure synthesis of diamond, although resulting in a lower thermal conductivity (<10 W/cm.K), has overcome the high cost of natural diamond. It is advantageous to deposit diamond on the backside of the device wafer so that heat dissipation is most effective and not hindered by the presence of other low thermal conductivity phases. However such a design of heat spreaders is not favored presently for two reasons. First, deposition of diamond at temperatures greater than 850°C leads to contamination and other reactions that are detrimental to further device processing and therefore special processing conditions have to be set up. Secondly, the low molar heat capacity associated with diamond makes it good for distribution of thermal energy rather than dissipation. Therefore, the lower heat capacity of diamond should be compensated by a higher heat capacity substrate on which diamond is deposited. This substrate with diamond layer on top is conveniently bonded to the backside of the device wafer.

Adhesion of diamond layer to the substrate is an important factor in the design of the heat spreader. When a high frequency power device is active, the heat spreader is subjected to heating and cooling cycles giving rise to residual thermal stresses that alternate. The adhesion of the diamond film to the substrate when subjected to the alternating stresses strongly depends on the strength of the interface and in order to improve the interfacial strength, multilayer diamond coatings have been developed [13]. In this new design, an intermediate layer of AlN is deposited embedding the discontinuous layer of diamond on the high heat capacity substrate and finally a continuous layer of diamond is deposited on the top for heat spreading. The choice of AlN as an intermediate layer is based on the high thermal conductivity of AlN (3.7 W/cm.K), matching thermal expansion coefficient (4.1×10^{-6}/K) with that of diamond ($3.1 \times 1 \times 10^{-6}$/K), high dielectric constant (8.8) and ease of deposition of AlN by reactive magnetron sputtering or pulsed laser physical deposition which is described at length in a recent reference [14]. Silicon carbide, also with a high thermal conductivity (5 W/cm.K), matching thermal expansion coefficient (4.3×10^{-6}/K), and high dielectric constant (9.0) is definitely suitable but deposition of high quality silicon carbide, hitherto, has been difficult at temperatures wherein diamond is stable. In addition, our previous attempts to deposit silicon carbide by laser PVD or magnetron sputtering at a substrate temperature of 600° to 800°C resulted in microcrystalline or amorphous phases.

3. Experimental procedure

3.1. Deposition of diamond and multilayer diamond for heat spreader substrates

Molybdenum or silicon nitride substrates of size 2.5 cm × 2.5 cm × 0.2 cm were used in the deposition of diamond film. Details of deposition conditions for diamond by microwave plasma chemical vapor deposition (MPCVD) are given in earlier reference [13]. Single layer diamond films consisting of diamond only were obtained by deposition for 8 hours. The thickness of the diamond films after 8 hours of deposition was found to be 10 to 12 μm. Multilayer diamond films consisting of diamond/aluminum nitride/diamond were deposited in a two-stage process. The first layer in this structure is a discontinuous layer of diamond deposited for 2 to 3 hours so that diamond crystallites of size 3 to 4 μm were separated by 1 to 2 μm. The substrate with discontinuous diamond is transferred to another chamber for deposition of AlN by laser physical vapor deposition (LPVD) or reactive magnetron sputtering (RMS). The details of deposition conditions for AlN are provided in our previous refernce [14]. Diamond suspension with 0.25 μm size crystallites was again provided on these substrates containing discontinuous diamond and AlN layers and a new continuous diamond layer was deposited for 10 to 12 hours. The parameters for diamond deposition were kept same for all diamond substrates prepared in this work. The total thickness of the multilayer coating consisting of the discontinuous diamond, intermediate layer of AlN and the top continuous diamond film was determined to be 14 to 16 μm. To enable the preparation of cross-sectional specimens that are used in the characterization of different layers, prototype samples were prepared under identical conditions by use of silicon (100) substrate in addition to molybdenum and silicon nitride.

3.2. Metallization of diamond surface and backside of silicon wafer

To provide good bonding between device wafer of either silicon or gallium arsenide and the diamond heat spreader substrate, metallization of the top surface of the diamond and the backside of the device wafer was used. Choice of the metallization layers was based upon the following four factors. First, adhesion to the diamond substrate is important. Second, it should not form an interfacial thermal barrier layer between the diamond and the solder layer used for the bonding. Third, wetting of the metallization layers with a higher thermal conductivity solder such as gold-tin eutectic alloy is essential for the bonding. Finally, there should be no void formation along the interface upon bonding to the diamond substrate. The metallization layers on diamond consisted of titanium and gold each deposited sequentially to a thickness of 0.10 to 0.15 μm and that of copper deposited to a thickness of 0.05 μm. Titanium is known to form a low resistance ohmic contact with diamond by formation of a carbide layer [15]. The second layer of gold followed by copper helped to wet easily with gold-tin eutectic solder. The details of deposition of metallization layers are given in our earlier reference [13]. Si(100) or GaAs(100) wafers were used

in the present work to bond to the diamond substrates. Both sides of the wafers were polished prior to metallization and cleaned chemically to remove the deformed layers. The metallization steps were different for backside of silicon and GaAs wafers. In the case of Si(100), a first layer of titanium followed by a second layer of gold and a final layer of copper were used. On the other hand, a first layer of copper-germanium alloy followed by a second layer of gold and a third layer of copper was used for the GaAs substrates. The thickness of the GaAs wafer specimen was only 100 μm whereas that of the silicon wafer was 500 μm. The copper-germanium alloy is with composition of Cu_3Ge that is used in the metallization of GaAs wafers.

3.3. Deposition of gold resistance heater on the front side of the wafer

Gold resistance heater of resistance between 200 to 250 ohms was deposited by laser PVD on the silicon wafer after it was bonded to diamond heat spreaders. Two leads to input constant power and the other two to measure current and voltage drop across the heater were used. Power input in the form of a pulse was given and temperature changes over the surface of the wafer were recorded continuously with time using an infrared imaging camera. Similar measurements were performed at different values of power input and the slopes of linear variation of temperature with time were calculated. The temperature of a fixed point on the wafer along a line perpendicular to the heater was used in these determinations. It should be mentioned that these do not represent steady state conditions.

3.4. Bonding the device wafer to the diamond substrates

Silicon wafers either with or without the resistance heater on the front side were bonded to three different heat spreader substrates, i.e. bare molybdenum, single layer diamond on molybdenum and multilayer diamond deposited on molybdenum. Similarly silicon wafers were bonded to the single layer diamond and the multilayer diamond deposited on silicon nitride. Also, GaAs wafers specimens of 100 μm thickness were bonded to the single layer diamond and the multilayer diamond deposited on the molybdenum substrates.

Gold-tin eutectic solder (80Au, 20Sn) was prepared in the form of a thin foil for bonding the device wafers to the substrates. A spring-loaded fixture was used to apply pressure between the wafer, solder film and the substrate assembly during bonding. This stainless steel fixture with the wafer, the solder and the substrate was placed in a chamber that was evacuated to 0.133 Pa and then hydrogen was introduced to an ambient of 266 Pa to prevent oxidation of the solder and the metallization layers, in particular, the copper layer. The assembly was taken slowly to a higher temperature (360°C) and was maintained at that temperature for 10 minutes. Cooling the assembly was carried out very slowly, at the rate of 2° per minute down to 150°C and at the rate of 4° per minute down to room temperature. The cooling rate was much slower ($<1°$ per minute) for bonding the GaAs wafer to the heat spreader to prevent failure of the wafer from residual thermal stresses that build up in the wafer due differences in thermal expansion coefficients.

4. Experimental results

In order to determine the suitability of the diamond heat spreaders for heat dissipation in the high frequency power devices, the bonded device structures were tested for different properties. Specifically, the specimens were tested for (a) adhesion strength, (b) resistance to failure against thermal cycling, (c) compositional uniformity and segregation in the bonded joint, and (d) heat spreader characteristics of the diamond substrates. The prototype samples and the wafer specimens bonded to the diamond films deposited on molybdenum or silicon nitride substrates were characterized and tested for evaluation of different characteristics of the bond.

4.1. Characterization of the single and the multilayer diamond films

The single and the multilayer diamond films deposited on the molybdenum and the silicon nitride substrates were characterized by X-ray diffraction, scanning electron microscopy, and Raman spectroscopy. Results of X-ray diffraction of the single layer and the multilayer diamond films deposited on the molybdenum substrate are shown in Fig. 1. The presence of the molybdenum carbide layer between the diamond layer and the molybdenum substrate is inferred from the diffraction peaks. The multilayer diamond film, as shown by the X-ray peaks, contains aluminum nitride as an intermediate

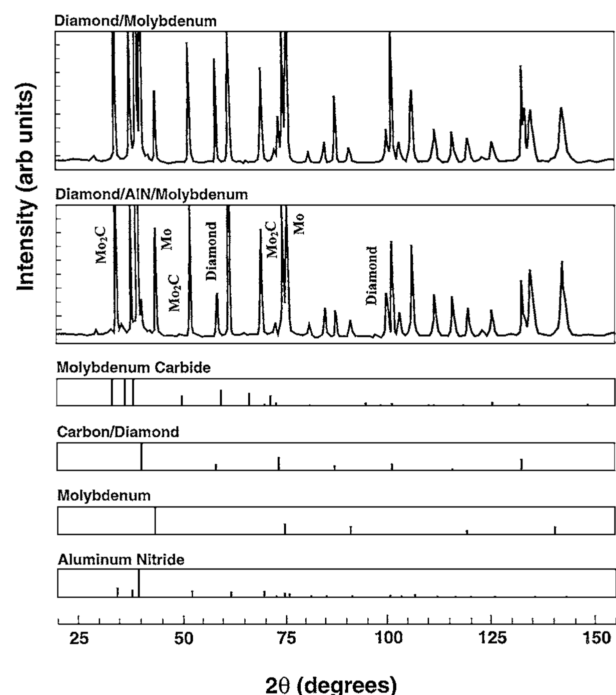

Figure 1 X-ray diffraction peaks associated with the single layer diamond film and the multilayer (diamond/AlN/diamond) film deposited on the molybdenum substrate. The positions of the peaks associated with the different regions in the pattern are shown below.

layer and molybdenum carbide between the diamond layer and the molybdenum substrate. The intensity of the AlN peaks is very weak because the thickness is very small. On the molybdenum substrate, the single layer diamond films of smaller thickness (12 μm) were found to be adherent, as shown in Fig. 2a. When deposition was continued to a larger thickness (25 μm), as shown in Fig. 2b, the diamond films were found to peel from the substrate upon cooling to room temperature from the diamond deposition temperature of

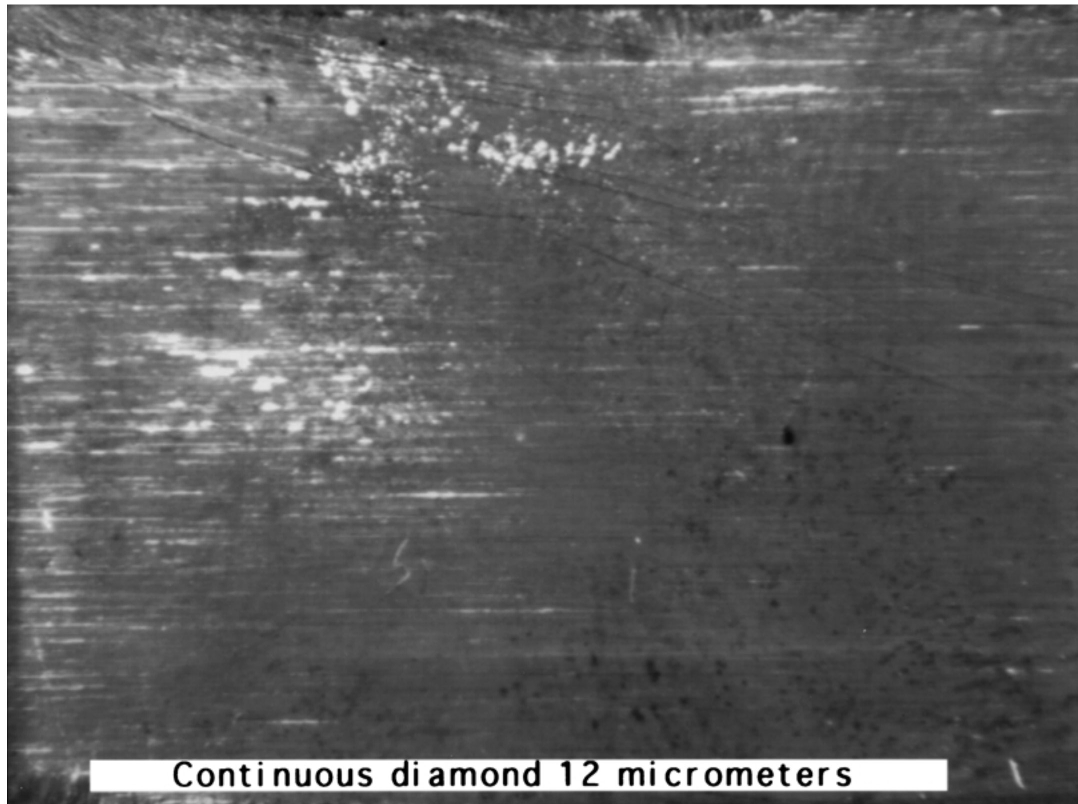

(a)

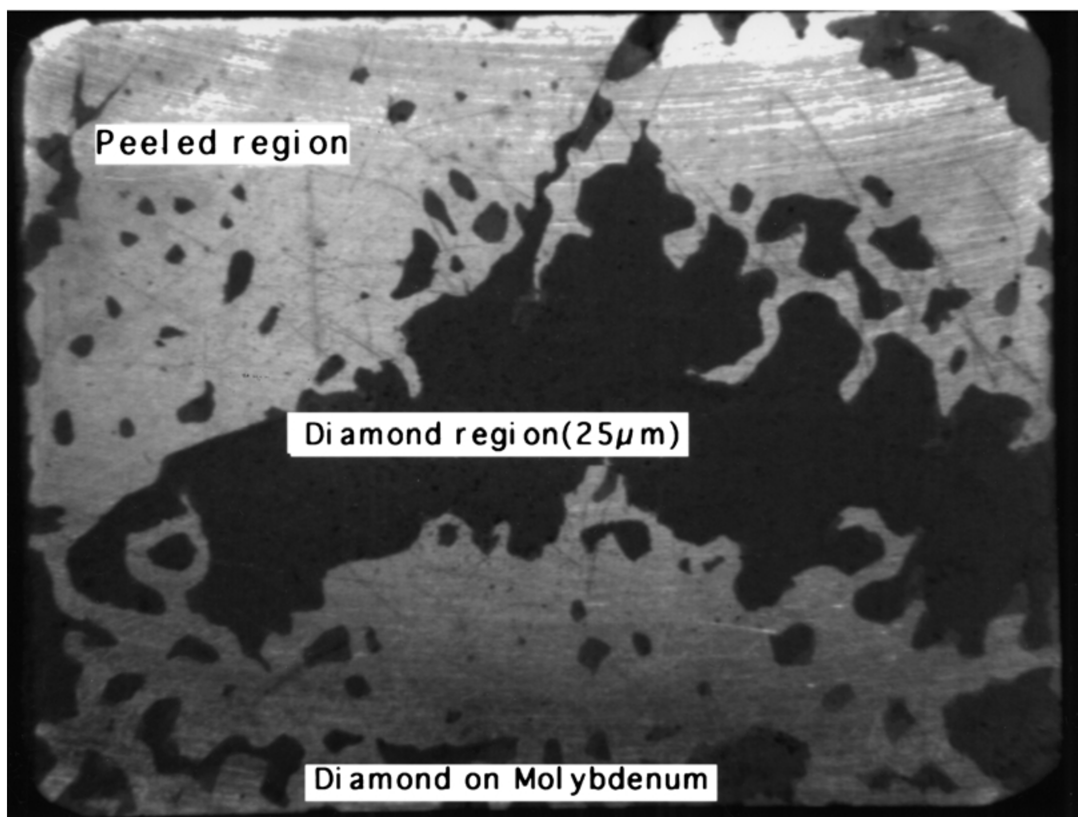

(b)

Figure 2 (a) Optical micrograph of the continuous single layer diamond film that maintained adhesion with the molybdenum substrate upon cooling from the deposition temperature of 900°C. (b) Optical micrograph of the continuous single layer diamond film that peeled from the molybdenum substrate upon cooling from the deposition temperature of 900°C.

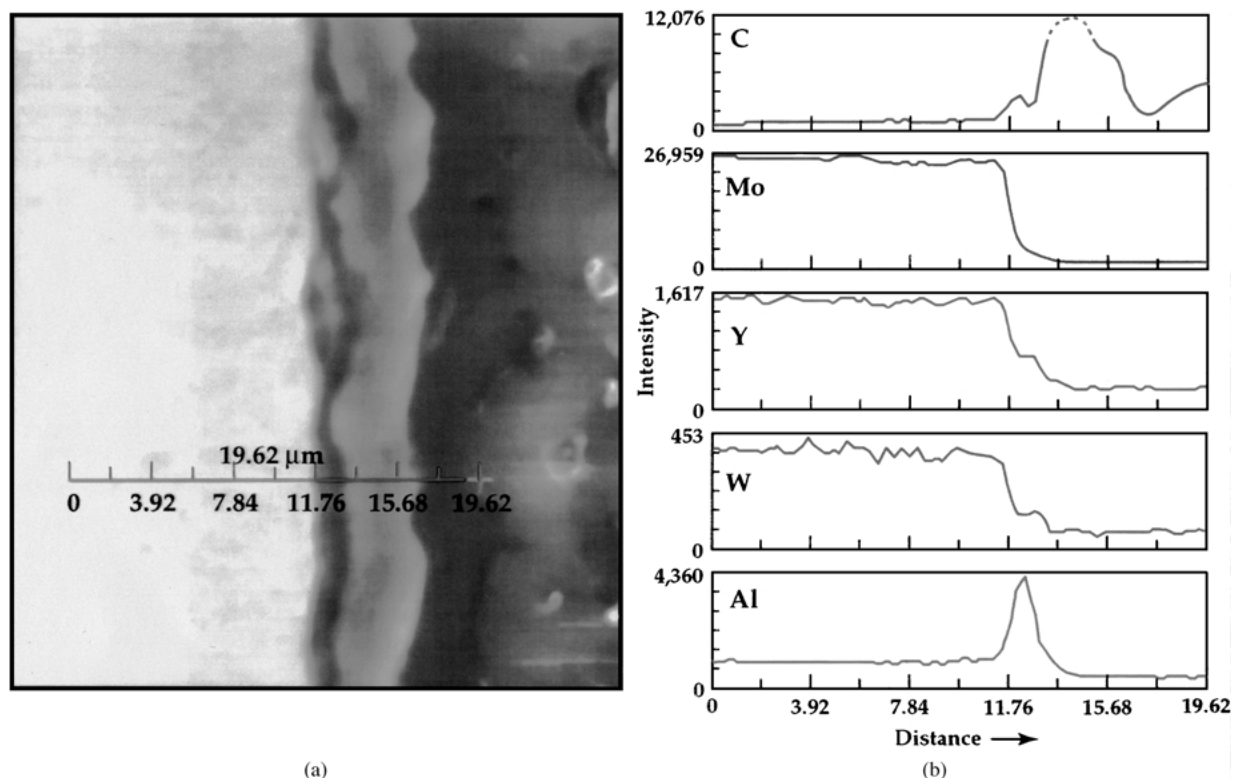

Figure 3 (a) Secondary electron image of the multilayer diamond film on molybdenum. (b) Elemental concentration line spectra across the multilayer structure corresponding to the scale marker in Fig. 3a.

900°C. On the other hand, the multilayer diamond films of thickness 16 μm maintained good adhesion. Fig. 3a illustrates the secondary electron image of the multilayer diamond coating and Fig. 3b gives the elemental concentration profile across the multilayer structure. The substrate signal consists of molybdenum with impurities of yttrium and tungsten. A small carbon peak associated with the discontinuous diamond layer followed by that of aluminum associated with the embedding AlN layer is seen. Finally, a large carbon peak associated with the continuous diamond layer is observed. These results show the presence of different layers of different thickness in the multilayer structure. Raman spectroscopy was used to characterize the single layer and multilayer diamond films. Fig. 4 shows the Raman spectrum associated the diamond film at different stages, namely (a) discontinuous film, (b) continuous film, (c) partially peeled continuous film, and (d) completely peeled film. The results clearly illustrate the absence of interfacial graphitic phase with peak close to 1585 cm^{-1} that is known to be responsible for delamination of diamond from the substrate [16]. Similarly, the diamondlike carbon peak is also not very strong. These spectra are indicative of high quality diamond film. Table I shows the position of the characteristic diamond peak observed in the different diamond films deposited on either molybdenum or silicon nitride substrates and the calculated values of residual stress using the familiar expression [17], $\sigma = C\ \mathrm{d}w/w$ where C is the biaxial modulus given by $2G(1+\nu)/(1-\nu)$, $\mathrm{d}w$ is the shift in the Raman peak from the characteristic equilibrium value, $w = 1332$ cm^{-1}, G is the shear modulus of diamond and ν the Poisson's ratio, giving $C = 1230$ GPa. The results clearly illustrate the build

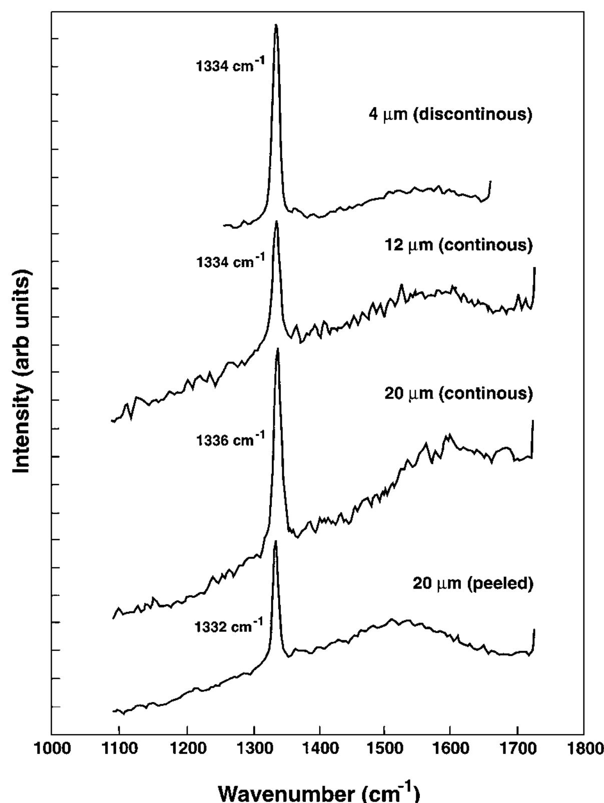

Figure 4 Raman spectrum associated with (a) discontinuous diamond film, (b) continuous diamond film, (c) multilayer diamond film, and (d) peeled diamond film from.

up of residual stresses in the single layer and the multilayer diamond film but the stresses are completely relieved in the peeled film. From these results it is concluded that whereas the residual stresses are not very

TABLE I Raman peaks associated with different diamond films deposited on molybdenum substrate and the calculated residual stresses

Film	Raman peak	Strain	Stress
Discontinuous diamond (4 μm thick)	1334 cm^{-1}	−0.0015	−1.846 GPa
Continuous diamond film (8 μm thick)	1334 cm^{-1}	−0.0015	−1.846 GPa
Continuous diamond film (18 μm thick partly peeled)	1336 cm^{-1}	−0.0030	−3.693 GPa
Multilayer diamond film (14 μm thick)	1335 cm^{-1}	−0.0022	−2.770 GPa
Diamond film peeled (18 μm thick)	1332 cm^{-1}	0	0

TABLE II Raman peaks associated with different diamond films deposited on silicon nitride substrate and the calculated residual stresses

Film	Raman peak	Strain	Stress
Discontinuous diamond (4 μm thick)	1334 cm^{-1}	−0.0015	−1.846 GPa
Continuous diamond film (8 μm thick)	1334 cm^{-1}	−0.0015	−1.846 GPa
Multilayer diamond film (10 μm thick)	1334 cm^{-1}	−0.0015	−1.846 GPa

much reduced in the presence of the intermediate layer of AlN, the adhesion strength of the multilayer film is increased, possibly by the reduction in the edge stresses and lowering of interfacial energy. Adhesion of AlN to molybdenum carbide is much better than that of diamond, and anchoring of diamond crystallites by AlN is thought to be responsible for improvement of adhesion strength [18]. We believe AlN provides anchoring of the diamond crystallites to the molybdenum carbide layer.

The single layer and the multilayer diamond films deposited on the silicon nitride were also characterized by X-ray diffraction and Raman spectroscopy. Results of X-ray diffraction showed the presence of different phases in the substrate and that of the diamond and the AlN layers. In contrast to the diamond films on molybdenum, absence of peeling of the diamond film from the silicon nitride substrate is an important feature and was further confirmed by the low residual stress in the diamond film that was evaluated from peak shifts observed in Raman spectroscopy. Results shown in Table II illustrate that the residual thermal stresses in the diamond layer are very small and these may be associated with the presence of point defects or free carbon atoms in the interstitial positions in the diamond lattice. Thus, diamond layer on silicon nitride substrate is promising and will be very useful provided the heat spreader characteristics are comparable to that of diamond layer on molybdenum substrate and also that the bond can withstand thermal cycling.

4.2. Characterization of the distribution of different elements in the bond

The changes in the distribution of different elements during bonding procedure at 360°C are important so that the accompanying variations in the adhesion strength of the bond can be understood. Cross-section specimens prepared from prototype samples, described in Section 3.1, were used for this purpose.

4.2.1. Silicon wafer bonded to diamond layer deposited on silicon wafer substrate

Fig. 5 illustrates the scanning electron microscopy (SEM) cross-section image of the bonded region with the diamond film, the gold-tin solder region and the silicon wafer on either side. The interface is very clean with the absence of observable segregation of any major phase and no void formation. The distribution of different elements in the metallization layers and the solder layer is analyzed by X-ray mapping and energy dispersion spectroscopy (EDS) and the results are also shown in Fig. 5. Silicon wafer is present in the extreme right and left sides of the bond. Diamond layers represented by carbon are present on silicon with no other intermediate layers. Upon bonding at 360°C for 10 minutes, the metallization layers of titanium and copper are redistributed uniformly in the solder region, as shown by X-ray mapping. It is also seen that silicon from the device wafer on the right diffused into the solder alloy to some extent. More significantly, carbon from the diamond layer has not shown significant diffusion into the solder region. Thus, the metallization layers and the solder region have merged into one region.

4.2.2. Silicon wafer bonded to diamond layer deposited on silicon nitride

Fig. 6 shows the SEM image and the X-ray maps of different elements in the solder region. High silicon signal on the right from the silicon nitride substrate, Cu, Sn, and Au signals in the middle, and silicon signal on the left from the bonded wafer are seen in the images. Carbon signal from the diamond layer was weak in the X-ray maps because it was not exposed to the irregularly cut surface. However, the SEM image illustrates the presence of the diamond layer. The presence of sharply defined boundaries from different regions is a clear indication that inter-diffusion during bonding at 360°C is limited to the liquid solder region and as a result no segregation of the metallization layers is present.

4.2.3. Gallium arsenide wafer bonded to diamond on molybdenum

Cross-sectional SEM micrograph and X-ray maps of different elements are shown in Fig. 7. Fig. 8 presents the results of EDS analysis of the bonded region showing the peaks associated with different elements. X-ray yield from copper and germanium in the metallization layers are weak and could not be shown. The larger width of various regions seen in the SEM and X-ray maps arises from the cross-sectional surface prepared by polishing at 11 degrees to the wafer surface so that a large area is exposed for analysis. The presence of gold in the eutectic solder and in the metallization layer on diamond forming two separate regions is seen in the

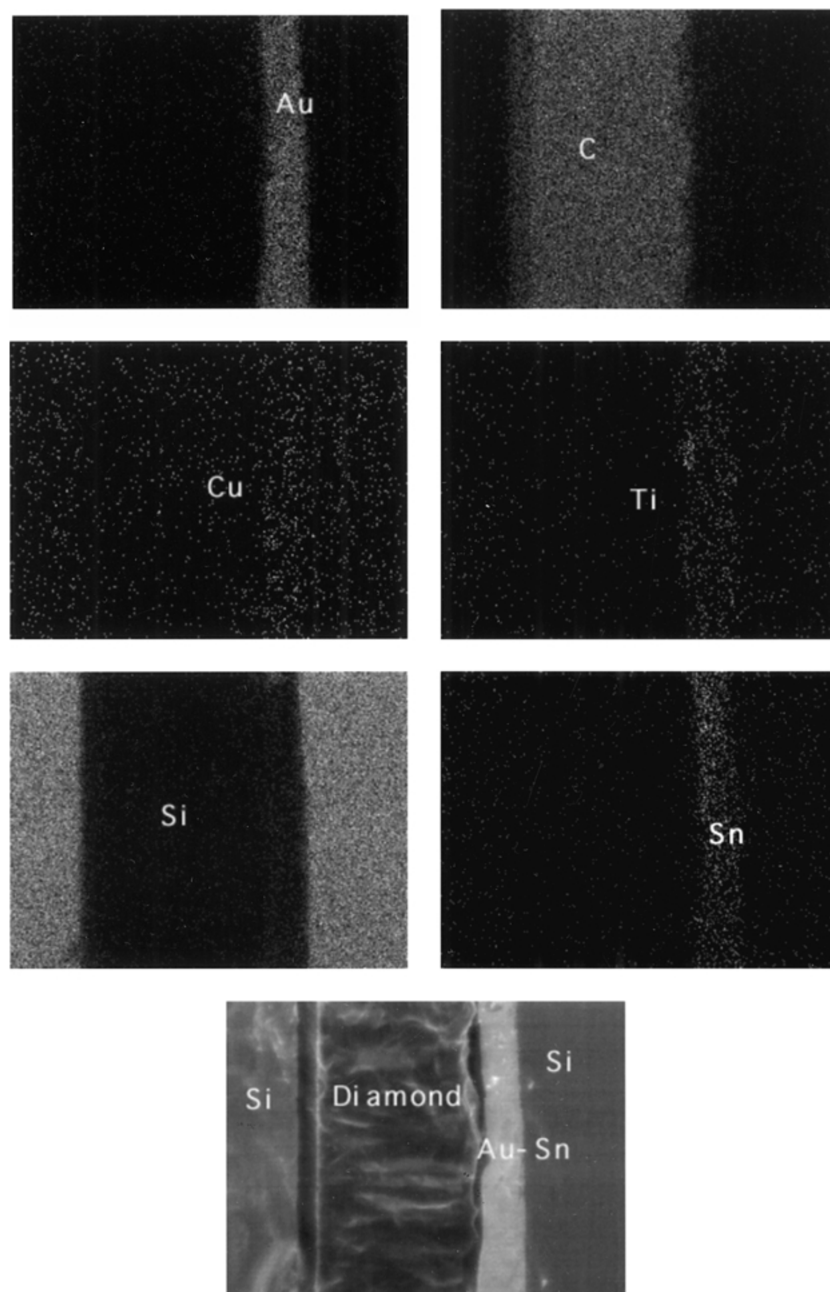

Figure 5 SEM micrograph of the prototype sample showing cross-section of the bonded silicon wafer to diamond layer deposited on silicon. The different layers in the cross-section are labeled.X-ray maps of Au, C (diamond), Cu, Ti, Si, and Sn in the cross-section image of the bond are also shown.

X-ray maps of gold. The large concentration of gold compared to that of tin in the eutectic solder is an indication of Au : Sn ratio equal to 4. The sharp interface between the GaAs wafer surface and the gold-tin eutectic solder region illustrates that inter-diffusion of gallium and arsenic into the eutectic solder region is restricted by the copper-germanium metallization layer which is very thin. Similarly, the titanium metallization layer limits inter-diffusion of carbon from the diamond layer into the eutectic region.

4.2.4. Adhesion strength of the bond between device wafer and heat spreader

Adhesion strength was determined by the pull test of the wafer specimens bonded to the diamond films deposited on different substrates. Brass rods of 4 mm diameter were glued on either side of the bonded wafer specimens using an epoxy bond of highest strength. In order to prevent any applied shear stress component on the bond, completely flexible steel cables were used to pull the bonded wafers in tension. The adhesion strength of the bonded wafer was found to be higher than that of the epoxy in all specimens. However a small number of samples of the diamond film deposited on silicon substrate failed by delamination along the diamond/titanium interface. The observed lower interfacial strength was thought to arise from graphitization of diamond surface at 600°C when titanium deposition was started. Metallization layer of titanium when deposited on the diamond film is found to form a carbide layer that exhibited a strength value of 5 Mpa. Improved deposition of titanium with better predeposition

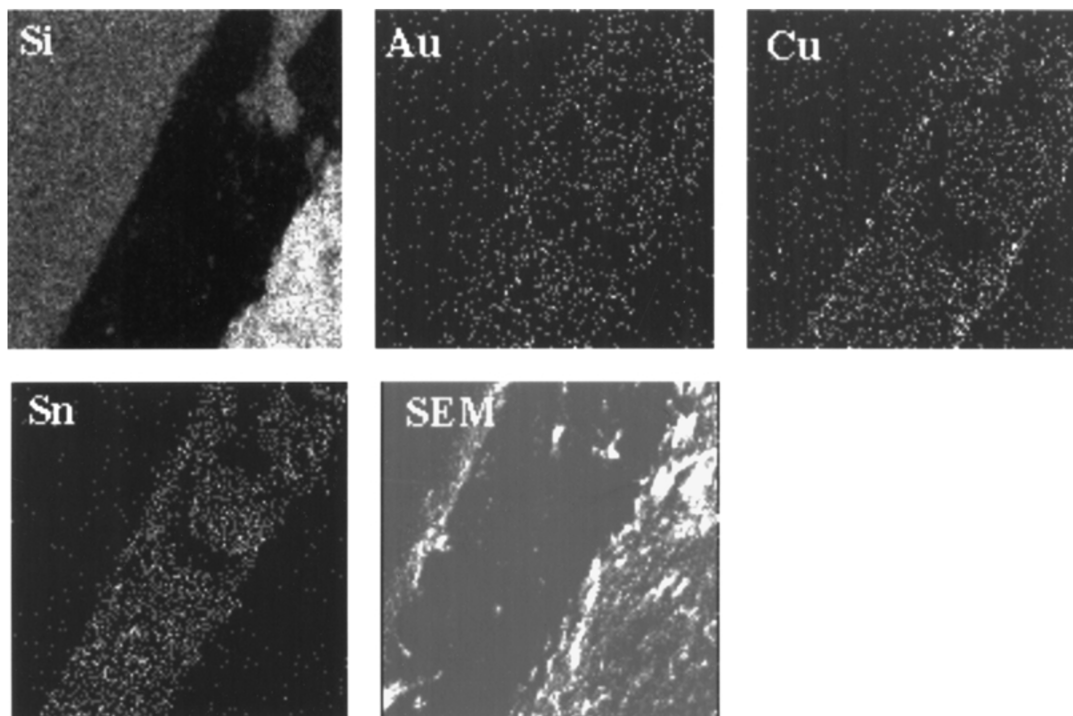

Figure 6 Cross-section SEM image and the X-ray mapping of elements Si, Au, Cu, and Sn in the silicon wafer bonded to silicon nitride substrate after thermal cycling between 25°C and 150°C.

vacuum and introduction of nitrogen atmosphere while raising the temperature of the diamond to 600°C to prevent the formation of the graphitic layer were chosen to improve the adhesion of titanium to diamond. Failure of the bonded wafers under impact was also investigated by dropping the bonded wafers from 2 to 3 ft high on a steel table. While the 500 μm thick silicon wafer bonded to the diamond layer on the molybdenum substrate or on the silicon nitride substrates withstood the impact, failure of the GaAs wafer bonded to the diamond layer on the molybdenum substrate by cleavage occurred because the wafer was very thin (100 μm).

4.2.5. Thermal stability of the bond

Thermal stability is the most important test for heat spreaders bonded to electronic power devices. Failure of the bond makes the heat spreader ineffective allowing the device temperature to increase. Failure can take place either under thermal fatigue or by cleavage at lower temperatures because the solder becomes brittle. Therefore, we have carried out three types of thermal cycling tests. In the first, thermal cycling was performed for 200 cycles between 20° to 150°C in a test apparatus with nitrogen ambient. A resistance heater was powered for half the cycle consisting of heating and turned off for the other half for cooling. In the second, thermal cycling test was performed between −20° to 150°C. For this type of test, after heating from room temperature to 150°C and cooling back to room temperature, further cooling to −20°C was performed by placing the specimen on a heavier copper block and by immersing it in dry ice and salt mixture. The temperature of the copper block was measured using a thermometer. The test was continued by placing the copper block at room temperature so that the bonded wafer reaches room temperature slowly. Further heating cycle continued from room temperature to 150°C in the nitrogen ambient. This type of cycling was performed for 20 cycles. The third type of thermal cycling was performed on silicon wafer bonded to silicon nitride substrate by rapid heating and cooling between −20° and 150°C. The sample was placed on a hot plate maintained at 150°C and quenched to −20°C by placing in dry ice and salt mixture. This type of cycling was carried out for 5 to 10 cycles. The results from these three types of tests were not completely the same. Specimens subjected to the three cycling tests were further examined for the failure of the bond by optical and scanning electron microscopy (SEM). The cross-section samples were made to determine the presence of voids or cracks along the interface by SEM. Also, specimens subjected to thermal cycling were further tested by pull test to determine if the adhesion strength of the bond was reduced.

Results from the first type of thermal cycling test showed the bond to be very strong. The solder bond region has not failed either during the thermal cycling or in the pull test. SEM examination showed no void or crack formation along the bonded region. Fig. 9 shows the cross-section SEM image and X-ray mapping of different elements in the silicon wafer bonded to the silicon nitride substrate that was tested in slow cycling between −20° to 150°C. Again, no voids or cracks are observed along the interface. A weak aluminum signal from that of the aluminum nitride in the multilayer diamond and a strong aluminum signal from the binder in the silicon nitride on the right with the gold and the tin signals from the solder region are also seen in the X-ray maps. A small number of specimens tested under rapid thermal cycling (type 3) failed by delamination. The two surfaces of the delaminated region are examined under SEM and X-ray mapping for identification

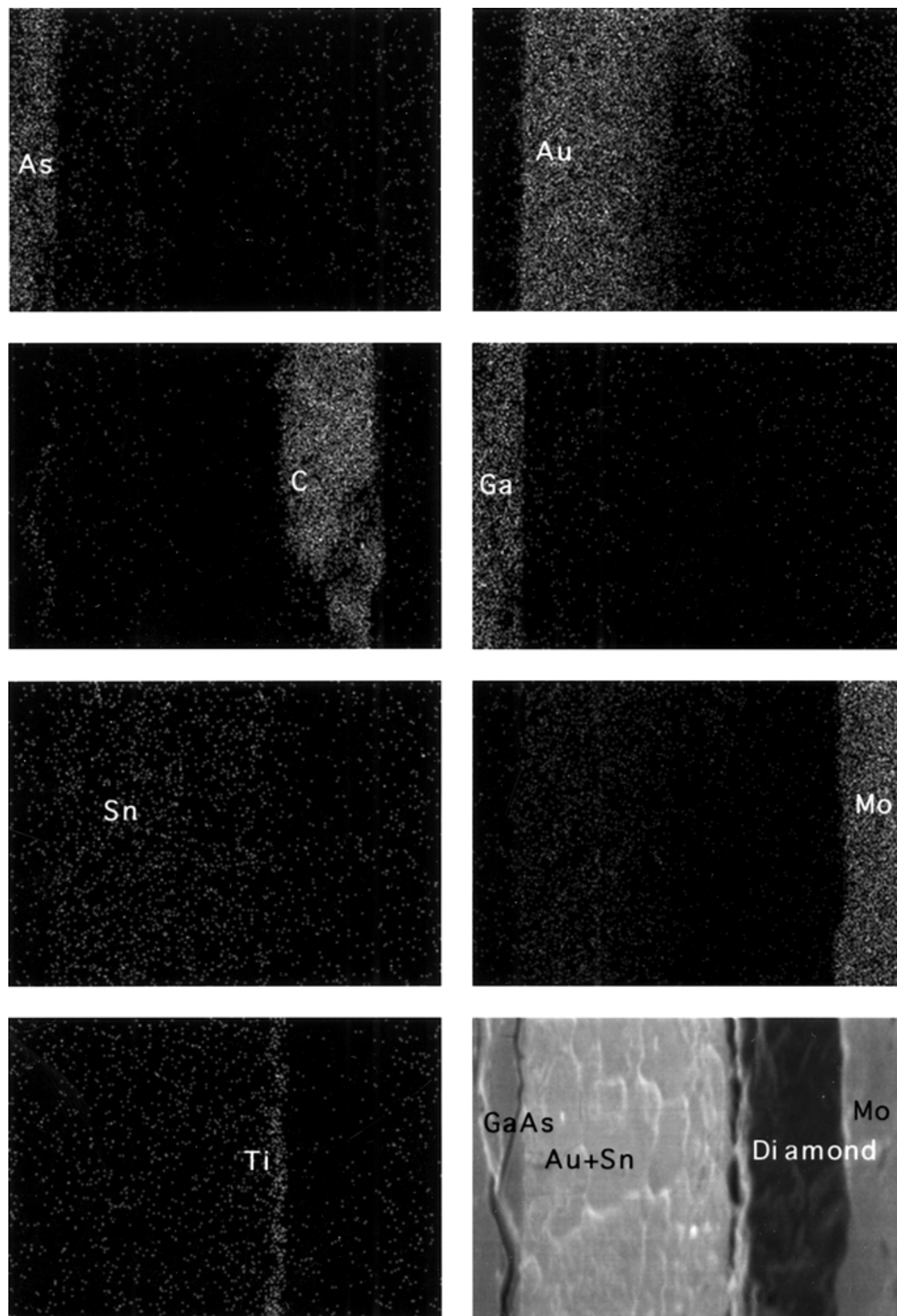

Figure 7 SEM micrograph of the cross-section of the sample of GaAs wafer bonded to diamond layer deposited on molybdenum. X-ray maps of Au, As, C (diamond), Ga, Mo, Ti, and Sn are shown.

of regions of void or crack nucleation and the results are shown in Fig. 10. The distribution of all the elements except Au,Sn, and Cu is uniform, as seen in the X-ray maps, but it is clear that the bond failed along the solder/diamond interface. The results also illustrate that there was no segregation of any elements in the solder region. The dark areas in the Cu signal coinciding with the regions in the Au and Sn signals and also in the SEM image illustrate the partial removal of the solder from the silicon wafer thus exposing silicon. Therefore, delamination is not a result of the presence of pockets of brittle solder. However, cleavage river patterns on the delaminated surface can arise when the solder region is very brittle at low temperatures. The solder region could not accommodate the high strain rate deformation associated with the rapid dimensional changes that resulted from the rapid decrease in temperature.

Thus, to summarize the results of thermal stability tests, slow cycling between room temperature and 150°C or between −20° to 150°C did not cause delamination along the bonded region. However, cycling with rapid heating and cooling was responsible for the delamination in certain samples which clearly illustrates that the high strain rate deformation resulting from quenching is responsible for the failure of the bond.

4.2.6. Heat spreader characteristics

The heat spreader characteristics of the single layer and the multilayer diamond substrates are compared with that of bare molybdenum substrates, as described in Section 3.3. The substrates are not cooled at the bottom of the heat spreader assembly; therefore, these experiments do not describe steady state conditions.

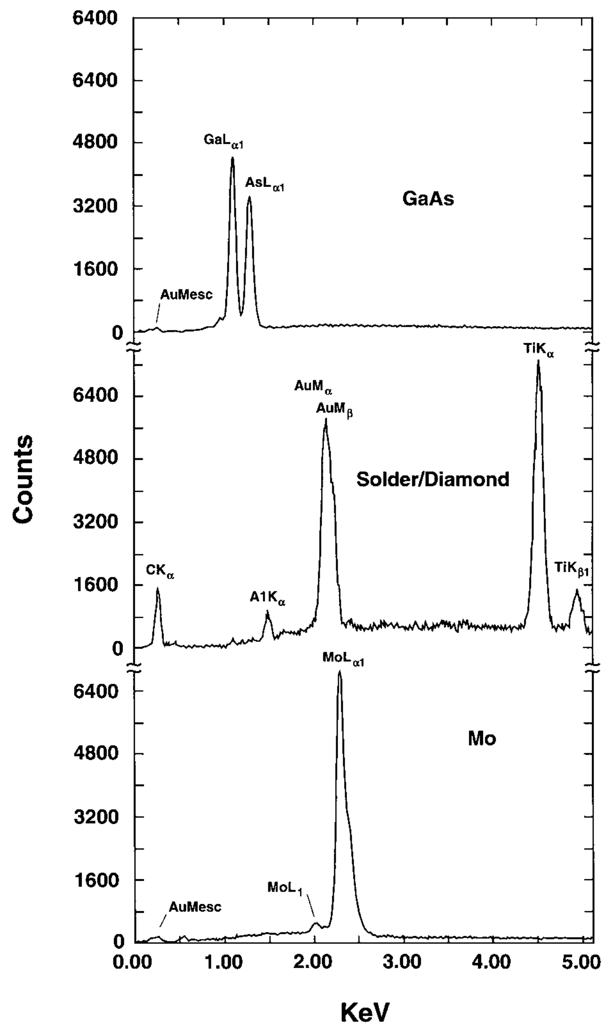

Figure 8 Energy dispersive X-ray analysis showing the peaks associated with Au, As, C (diamond), Cu, Ga, Ti, Sn, and Mo in the cross-section image of the bond shown in Fig. 11. Spectrum is obtained in the three regions of the bonded structure separately.

The rate of increase of temperature per unit power input remained almost constant up to a third decimal place in all specimens illustrating that it is independent of the value of the power input. The results of temperature rise for the three substrates used in this comparative study [18] are shown in Fig. 11. These results clearly illustrate that the multilayer diamond substrate bonded to silicon wafer has the highest heat spreader characteristics. In addition, the heat spreader characteristics of the single layer diamond substrate were lower than that of the multilayer diamond substrate and that of the bare molybdenum substrate are found to be the lowest. Thus, the present investigation clearly established that aluminum nitride embedding layer improved the adhesion, the thermal stability, and the heat spreader characteristics of the diamond layer on the molybdenum substrate.

5. Discussion

Residual thermal stresses developed between diamond layer and the molybdenum substrate are thought to be responsible for the delamination upon cooling from the deposition temperature of diamond (900°C). The presence of the molybdenum carbide layer between the diamond layer and the molybdenum substrate while providing good adhesion is also responsible for the thermal stresses because the thermal expansion coefficient of Mo_2C (5.8×10^{-6}/K) is higher than that of either molybdenum (4.9×10^{-6}/K) or the diamond film (3.1×10^{-6}/K). Residual stresses are seen to be equally high in the presence of the intermediate layer of AlN but the adhesion strength of the multilayer film is increased. An improvement in the adhesion strength may arise from the reduction in the edge stresses and lowering of the interfacial energy. Adhesion of AlN to molybdenum carbide has been found to be much

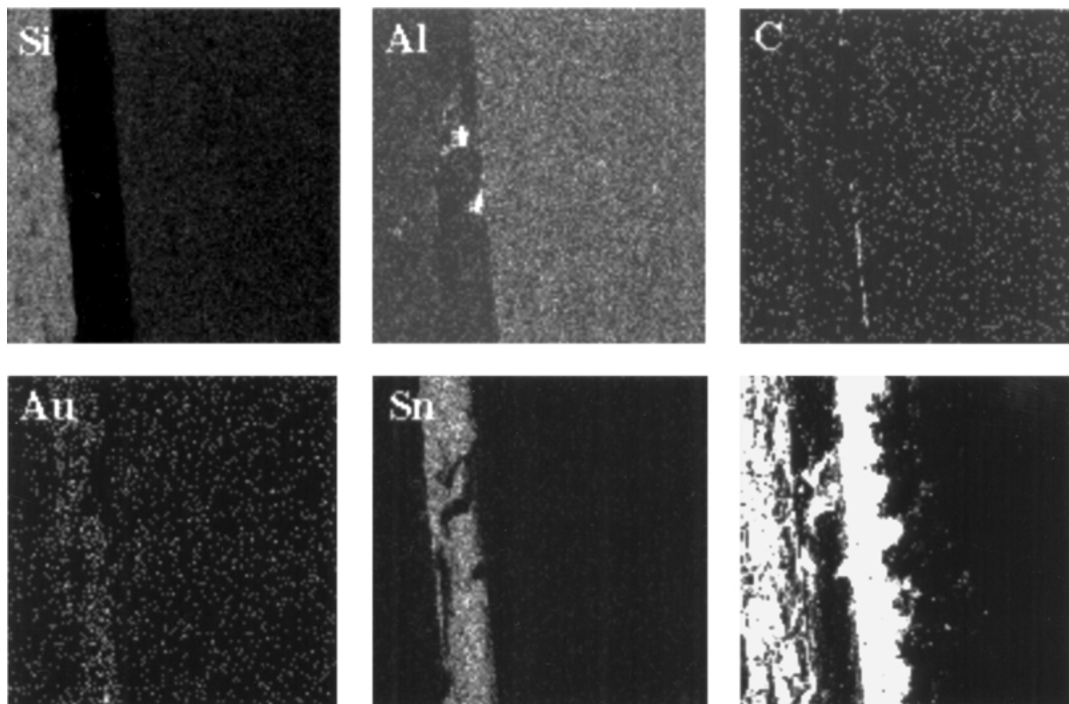

Figure 9 Cross-section SEM image and the X-ray mapping of elements Al, Au, C (diamond), Si, and Sn in the silicon wafer bonded to silicon nitride substrate after thermal cycling between −20°C and 150°C. The right hand side region is the silicon nitride substrate and the left hand side is the silicon wafer. Al signal on the right arises from the binder in silicon nitride. Irregular diamond region is seen next to the silicon nitride on the right.

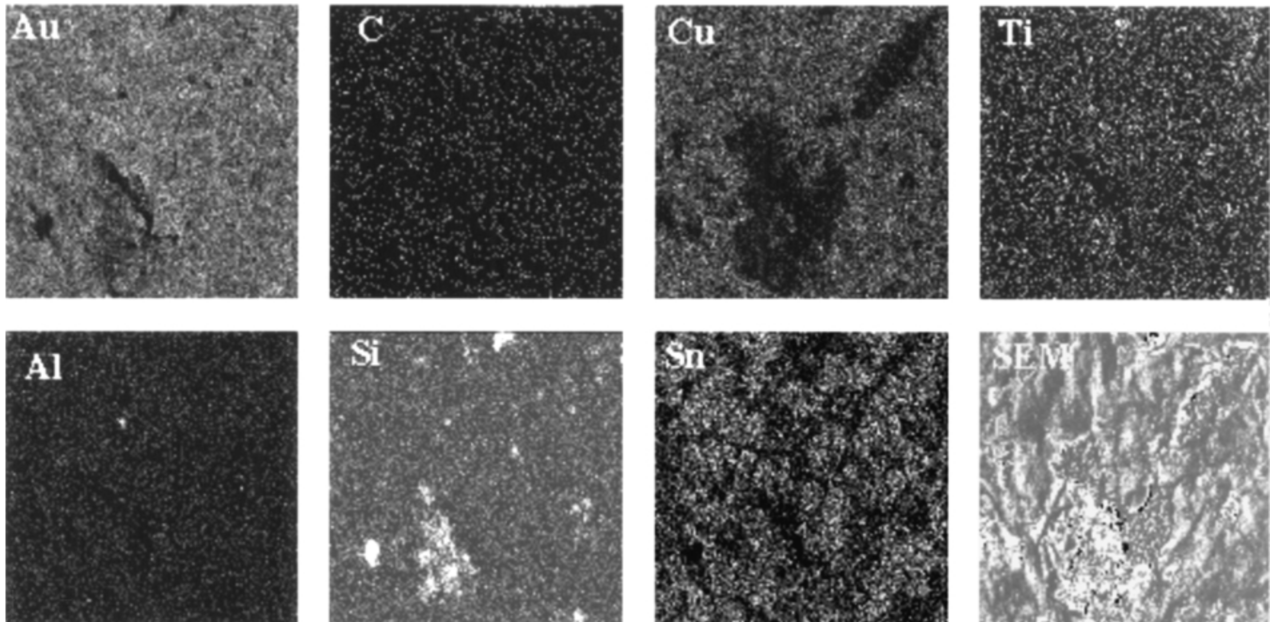

Figure 10 SEM image and X-ray mapping of Al, Au, C (diamond), Cu, Ti, Si, and Sn for identification of regions of voids or crack nucleation. X-ray maps show the presence of elements in the metallization layers and that of the elements in the solder region and very week signals of carbon.

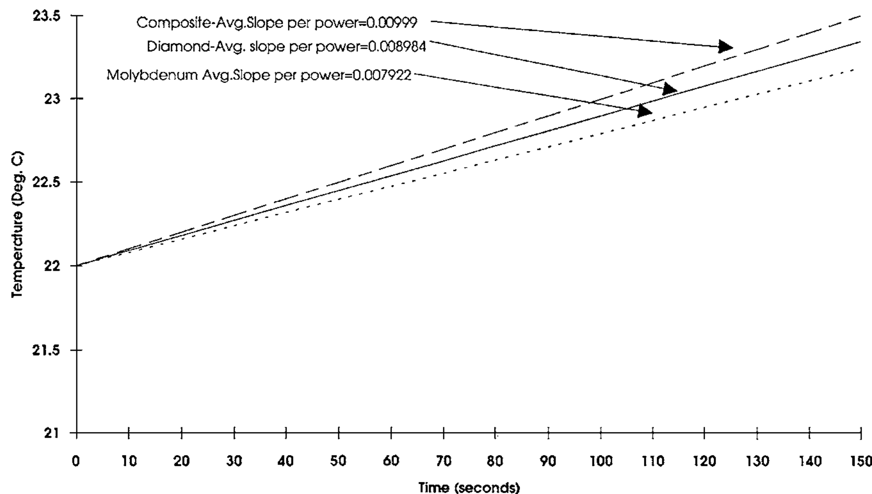

Figure 11 Results of IR imaging of silicon wafer bonded to diamond. Temperature at a fixed point measured along a line perpendicular to the heater line is plotted as a function of time. Average slope corresponds to that for three input power settings.

higher than that of diamond to molybdenum and therefore, anchoring of the diamond crystallites by AlN will be responsible for improvement of adhesion strength. The presence of the AlN intermediate layer thus serves either to reduce the interfacial energy or to increase the bond strength because AlN exhibits better bond strength to the molybdenum substrate. Secondly, mechanical interlocking and reduction of edge stresses are thought to be responsible for the improvement of the adhesion of diamond layers. Finite element modeling (FEM) of thermal stresses [19] has shown that the edge stresses are reduced in magnitude. Further, it is also found through FEM that the stresses alternate in the multilayer structure whereas these become compressive in the single layer diamond film leading to buckling. As a result, cracks nucleated along the edges can not propagate into the region under compressive stresses. Therefore, it is concluded that this improvement in the adhesion of diamond to the high heat capacity substrate is an important contribution to the development of heat spreaders that will withstand thermal cycling.

The effective thermal conductivity of diamond heat spreader is not reduced greatly by the interfacial layers of titanium and titanium carbide because these are very thin (0.5 μm). Metallization layers on the backside of the device wafers similarly reduce the effective thermal conductivity, but also provide the ability of the bond to withstand temperature changes. In particular, titanium, gold and copper layers on the backside of silicon are ductile, and can by plastic relaxation, accommodate the dimensional changes arising from the differences in the thermal expansion coefficients. Similarly, the choice of the metallization layers consisting of gold, copper-germanium alloy and copper on the backside of gallium arsenide wafer is based on the ability of

these layers to plastically deform and accommodate the dimensional changes during cooling from the bonding process temperatures.

Characterization of the bonded wafers to the diamond substrate using SEM and X-ray mapping clearly illustrated that the metallization layers diffused in to the liquid solder forming a single region. This result is readily seen from the X-ray maps wherein titanium signal is confined close to the diamond whereas that of all the other metallization layers such as copper is included in the solder. Diffusion of the metallization layers into the solder illustrates that the interface is graded and such interfaces exhibit higher strength than the interfaces with sharp changes in concentration. Finally, diffusion of silicon from silicon wafer or gallium and arsenic from GaAs wafer into the solder region illustrates that a diffusion bond has formed with the wafer. Similarly, the observed diffusion of titanium from the metallization layer on the diamond layer into the solder, seen in the X-ray maps, illustrates that the strength of the bond arises from the diffusion bond to the diamond layer. The toughness and ductility of the bond depends on the ability of the solder to deform plastically. Eutectic gold-tin solder forms a brittle microstructure that could be responsible for observed cleavage failure at lower temperatures and high strain rates. The presence of excess gold in the eutectic can increase the ductility of the eutectic solder and thereby prevent the cleavage failure. Thus, to prevent bond failure along the eutectic solder, we believe a gold rich solder composition will be advantageous.

Thermal stability of the bonds formed between the diamond heat spreader and the silicon or the GaAs wafer has been found to be excellent when the cycling is carried out slowly between room temperature and 150°C or between −20° and 150°C. Cross-section microscopy carried out after subjecting the bonded wafers to thermal cycling illustrated that no voids or cracks are present along the interface. On the other hand, failure of the bond upon rapid thermal cycling illustrates that crack or void nucleation has occurred. Crack nucleation takes place from centers such as voids formed during reaction of the solder with the metallization layers. Either because of differences in specific volume of different microstructural constituents or because of volume changes in certain phases resulting from the temperature change, formation of voids is expected. SEM examination of the delaminated surfaces has not showed the presence of voids or cracks along the interface. We believe excess quantities of tin in the solder can lead to regions of free tin that are responsible to volume contraction. Tin undergoes a polymorphic transformation at 13°C from the diamond cubic to body centered tetragonal phase accompanied by a volume contraction of 27%. Such volume changes associated with any regions of free tin phase will be responsible for void nucleation. We have not been able to detect any segregation or excess form of tin in the solder region and therefore, there is no conclusive evidence to the presence of free tin. However, formation of river patterns from cleavage crack propagation, as shown in Fig. 12, indicates that nucleation has been initiated at certain regions of stress concentration in the solder. Since only a small fraction of the specimens subjected to rapid temperature cycling failed, we believe improvement of solder properties by introduction of a more ductile phase, such as gold, in the solder is essential to improve the toughness at high strain rates of deformation arising from rapid cooling. Results of these experiments with slightly higher concentration will be presented subsequently. It must be pointed out that the melting of the gold rich solder takes place over a larger range of temperatures, much higher than the eutectic temperature and this factor is not very favorable for bonding.

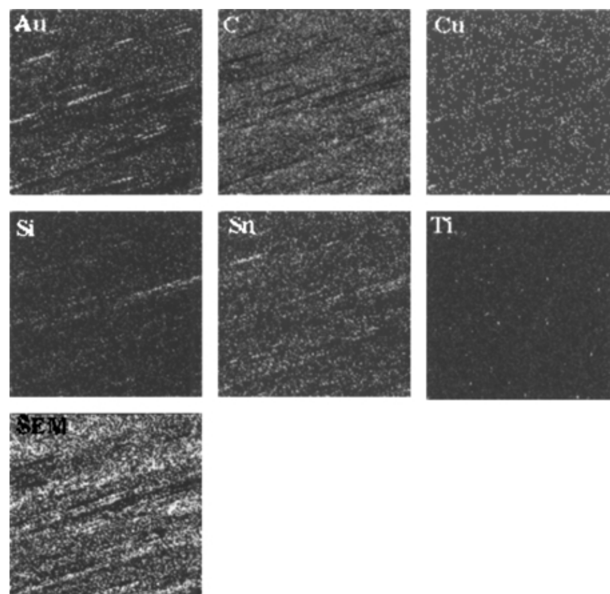

Figure 12 X-ray mapping of different elements on the bond side of the silicon wafer with metallization layers taken after the bond peeled due to quenching to ice/salt temperature. Formation of river patterns due to cleavage are seen.

The heat spreader characteristics of the single layer and the multilayer diamond on the molybdenum substrate have clearly shown that the multilayer diamond films are better than the single layer diamond as well as the bare molybdenum substrates. Two parameters responsible for dissipation of the thermal energy are (a) the thermal conductivity of the medium and (b) the specific heat of the heat spreader. Because we are interested in the performance of the hear spreaders in the absence of steady state conditions and for the high frequency power devices, specific heat also becomes an important factor. It was shown by a detailed analysis of the effective thermal conductivity of polycrystalline diamond and diamond/AlN/diamond composites [13, 20] that when AlN phase fills the void space in the diamond layers deposited in the laboratory, the effective thermal conductivity is improved. Polycrystalline diamond films deposited in the laboratory contain microscopic voids or diamondlike carbon both of which possess very low thermal conductivity [21] and therefore, offer large thermal barrier resistance. An interfacial layer of diamondlike carbon of few atomic layers is found to exist between diamond crystals by high resolution transmission electron microscopy. When heat flow takes place perpendicular to the interface containing the void or diamondlike carbon regions, the effective thermal

conductivity is drastically reduced. On the other hand, AlN layer becomes the interfacial phase by replacing the diamondlike carbon regions and thus, helps to improve the effective thermal conductivity.

The effective thermal conductivity K_e of diamond/AlN/diamond when heat flow takes place normal to the interface, in the absence of any thermal barrier resistance [13, 20], can be written in the form,

$$1/K_e = \{f_{DLC}/K_{DLC} + f_{AlN}/K_{AlN}\}v_f + v_C/K_C$$

where K's represent the thermal conductivities and v's the volume fractions of different phases, $f_{DLC} = v_{DLC}/v_f$, $f_{AlN} = v_{AlN}/v_f$, and $f_{DLC} + f_{AlN} = 1$ and $v_{DLC} + v_{AlN} + v_C = 1$. The terms with subscripts represent C for diamond, AlN for aluminum nitride and DLC for diamondlike carbon. Thus, v_f is the volume fraction of the interfacial phase either in the form of diamondlike carbon or aluminum nitride and the values of f with subscripts DLC or AlN represent the fraction of the interfacial phase either diamondlike carbon or aluminum nitride, respectively. The above equation is applicable when heat flow takes place across the interface between diamond grains. In the absence of proper determination of thermal conductivity of CVD diamond in our experiments, we have assumed the thermal conductivity of diamond $K_C = 20$ W/cm.K, that of AlN, $K_{AlN} = 3.7$ W/cm.K, and that of diamondlike carbon, $K_{DLC} = 2$ mW/cm.K [21] for illustrative purposes. We have calculated the effective thermal conductivity of the composite by choosing a value of v_f and varied the value of f_{DLC} and therefore f_{AlN} from 0 to 1. The results shown in Fig. 13 illustrate that the effective thermal conductivity decreases for higher value of fraction of the total interfacial phase and also of the fraction of the diamondlike carbon. For example, the effective thermal conductivity decreases to 2 W/cm.K when the volume fraction of diamondlike carbon along the interface is 0.01 whereas it decreases to 14 W/cm.K when the volume fraction of AlN is 0.1. We have not included the interfacial thermal barrier resistance that will further reduce the effective thermal conductivity.

The improvement in the effective heat capacity of the substrate when different volume fractions of AlN layer replace the diamondlike carbon is given by

$$Q/V = mC_p\Delta T/V = \{v_C\rho_C C_{pC} + v_{AlN}\rho_{AlN}C_{p\,AlN} + v_{DLC}\rho_{DLC}C_{DLC}\}\Delta T$$

where as before $v_C + v_{AlN} + v_{DLC} = 1$, Q represents the heat absorbed per unit volume, V of the composite, v's represent the volume fraction, ρ's represent the density and C_p's represent the specific heat. The value of Q/V, shown in Fig. 14, as a function of different volume fractions of the interfacial phase, either in the form of AlN or diamondlike carbon, increases with the volume fraction of AlN. However, it decreases when diamondlike carbon replaces the AlN phase. These results clearly illustrate that replacement of diamondlike carbon with AlN improves both the effective thermal conductivity and the heat absorbed per unit volume of the film. Thus, the multilayer composite coatings of diamond/AlN/diamond exhibit better heat spreader characteristics than the single layer diamond coatings because the AlN film replaces the diamondlike carbon or the voids in the diamond layers deposited by low pressure synthesis. The diamondlike carbon or the voids are known to form along the interfaces because of the three-dimensional nature of growth of diamond in the lower pressure synthesis.

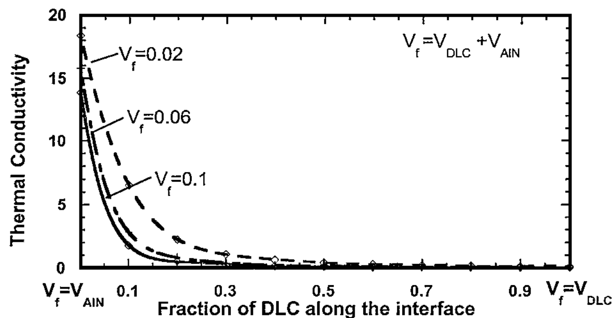

Figure 13 Calculated values of the effective thermal conductivity associated with the diamond/AlN/diamond composites shown as a function of the fraction of the diamondlike carbon or that of AlN. Different values of the volume fraction of interfacial phase either in the form of diamondlike carbon or AlN are chosen. For a given value of the volume fraction of the interfacial phase, that of diamondlike carbon or AlN is changed.

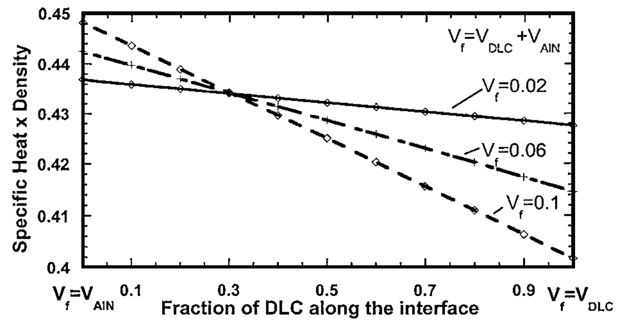

Figure 14 Calculated values of the heat absorbed by the diamond/AlN/diamond composite shown as a function of the fraction of the diamondlike carbon or that of AlN. Different values of the volume fraction of interfacial phase either in the form of diamondlike carbon or AlN are chosen. For a given value of the volume fraction of the interfacial phase, that of diamondlike carbon or AlN is changed.

6. Summary and conclusions

A novel design of the heat spreaders for high power electronics is presented. Bonding of the device wafers to the heat spreader using different metallization schemes and gold-tin eutectic solder has been found to maintain good adhesion, resistance against peeling under rapid thermal cycling and provide better heat spreader characteristics compared to a single layer diamond or bare molybdenum heat spreader. Characterization of the bonded region showed that the strength of the bond arises from the diffused regions of metallization layers in the solder and the ductile interfacial regions that can accommodate thermal stresses. The detrimental effect of diamondlike carbon phase on the effective thermal conductivity and the heat capacity of the multilayer diamond and single layer diamond is evaluated. Aluminum nitride embedding layer is shown to improve the heat spreader characteristics when DLC is replaced

by it in the multilayer composites. The following conclusions are reached.

1. The adhesion strength of the diamond layer to the high heat capacity substrates is very much improved by the presence of an embedding layer of aluminum nitride.

2. The metallization layers of titanium, gold and copper on the diamond layer or on the backside of the silicon wafer and that of titanium, copper-germanium alloy, and copper on backside of the gallium arsenide are found to provide the good bonding and the wetting with the gold-tin eutectic solder and also accommodate the thermal stresses.

3. The gold-tin eutectic solder with slightly excess gold is also thought to be better than the brittle eutectic composition to accommodate the thermal stresses.

4. The bonded device wafers are able to sustain the rapid thermal cycling provided the solder can withstand the high strain rate deformation.

5. The heat spreader characteristics of the multilayer diamond/AlN/diamond composites are found to be better than that of the single layer diamond.

6. The diamondlike carbon present in the diamond films deposited by chemical vapor deposition is detrimental to the heat spreader characteristics. Improvement in the heat spreader characteristics is achieved by replacement of the DLC phase with the higher thermal conductivity aluminum nitride.

7. The multilayer diamond films offer better heat spreader characteristics, adhesion properties, and resistance against thermal cycling so that life of the high frequency power devices is prolonged.

8. The improvement in the heat spreader characteristics of the multilayer diamond films is associated with the replacement of the microscopic voids or the diamondlike carbon in CVD diamond by AlN.

Acknowledgments

This research work is supported by Division of Design, Manufacture and Industrial Innovation of NSF, Assistant Secretary for Energy Efficiency and Renewable Energy, Office of Transportation Technologies as part of HTML User Program, ORNL, and South Eastern Universities Research Association, Inc.

References

1. O. M. KUTTEL, E. SCHALLER, J. OSTERWALDER and L. SCHLAPBACH, *Diamond Related Materials* **4** (1995) 612.
2. P. J. BOUDREAUX, in Applications of Diamond Films and Related Materials: 3rd Int. Conf., edited by A. Feldman *et al.*, NIST Special Publication 885 (NIST, Washington, DC, 1995).
3. S. ASHLEY, *Mech. Engng.* **112** (1990) 54.
4. W. BEHR and J. F. LUY, *IEEE Electron Device Lett.* **11** (1990) 206.
5. H. UKITA, H. NAKADA and T. ABE, *Jpn. J. Appl. Phys.* **31** (1992) 524.
6. G. LU and L. K. BIGELOW, *Diamond Related Materials* **1** (1992) 34.
7. J. E. GRAEBNER and S. JIN, *J. Metals* **50** (1998) 52.
8. K. E. GOODSON, in ASME/JSME Thermal Engineering Conference, 1995, Vol. 4, p. 183.
9. J. H. HARRIS, *J. Metals* **50** (1998) 56.
10. R. D. COTTLE, X. CHEN, R. K. JAIN, Z. ELIEZER, L. RABENBERG and M. E. FINE, *ibid.* **50** (1998) 66.
11. H. MAVOORI and S. JIN, *ibid.* **50** (1998) 70.
12. C. ZWEBEN, *ibid.* **50** (1998) 47.
13. K. JAGANNADHAM, *Solid State Electronics* **42** (1998) 2199.
14. K. JAGANNADHAM, A. J. SHARMA, Q. WEI, R. KALYANARAMAN and J. NARAYAN, *J. Vac. Sci. Tech.* **16**A (1998) 2804.
15. K. K. DAS, in "Diamond Films and Coatings," edited by R. F. Davis (Noyes Publications, Park Ridge, NJ, 1993) Ch. 8, p. 381.
16. B. LU and R. HAUBNER, in "Diamond and Diamond-like Films and Coatings," edited by R. E. Clausing *et al.*, NATO-ASI Series B: Physics Vol. 266 (Plenum, New York), p. 579.
17. T. R. WATKINS, A. MCGINNIS and K. JAGANNADHAM, in Proc. Advances in X-ray Analysis, Denver, Colorado, 1997.
18. K. JAGANNADHAM, W. D. FAN, R. B. DINWIDDIE and J. NARAYAN, in Symp. Proc. MRS Society, Boston, 1997, Vol. 445, p. 51.
19. W. D. FAN, K. JAGANNADHAM and J. NARAYAN, in Symp. Proc. MRS Society, Boston, 1995, Vol. 356, p. 847.
20. K. JAGANNADHAM, *J. Vac. Sci. Tech.* **17**A (1999) 373.
21. C. J. MORATH, H. J. MARIS, J. J. CUOMO, D. L. PAPPAS, A. GRILL, V. V. PATEL, J. P. DOYLE and K. L. SAENGER, *J. Appl. Phys.* **76** (1994) 2636.

Received 7 February
and accepted 13 November 2001